Nanostructure of Bioactive Sol−Gel Glasses and Organic−Inorganic Hybrids

María Vallet-Regí,*,† Antonio J. Salinas,† Julio Ramírez-Castellanos,‡ and José M. González-Calbet‡

Departamento de Química Inorgánica y Bioinorgánica, Facultad de Farmacia, and Departamento de Química Inorgánica. Facultad de CC, Químicas, Universidad Complutense, E-28040 Madrid, Spain

Received November 22, 2004. Revised Manuscript Received January 25, 2005

The nanostructure of three bioactive materials, two sol−gel glasses in the SiO_2−CaO and SiO_2−CaO−P_2O_5 systems and a SiO_2−CaO−poly(dimethylsiloxane) organic−inorganic hybrid, has been studied for the first time by high-resolution transmission electron microscopy. The nanostructural characterization indicates that the addition of P_2O_5 to the glass leads to crystallization of a silicon-doped calcium phosphate, while in the materials without any phosphorus content—binary glass and hybrid—calcium is located in an amorphous silica network. The different rates of positive bioactive response of both glasses (with and without phosphorus) are strongly correlated with their nanostructure since the distances between [SiO_4^{4-}] tetrahedra decrease when calcium is not present in the vitreous network and phosphorus bonds to calcium to form a silicon-doped calcium phosphate.

Introduction

The development of new bioactive materials able to bond to living tissues is a promising alternative for the production of implants and scaffolds for tissue engineering. Many bioactive materials are prepared by a sol−gel method, including glasses and organic−inorganic hybrids. When in contact with physiological fluids they form carbonated hydroxyapatite (CHA) nanocrystals similar in composition and structure to biological apatites. This was considered an essential stage in the formation of a bond between the bioactive glasses and the living tissues.[1] Likewise, bioactive materials also form CHA nanocrystals in vitro when immersed in solutions mimicking human plasma.[2] Throughout this study they shall be termed as bioactive those materials coated by an apatite-like layer after soaking in Kokubo's simulated body fluid (SBF).[3]

There are plenty of references in the literature which deal with the characterization of bioactive glasses,[4] albeit generally focused on their macrostructural characterization. To improve our knowledge of some questions related with the in vitro bioactivity of sol−gel glasses, such as why some compositions are bioactive or why the CHA formation rate depends on the composition, surface area, and porosity of glasses, a nanostructural characterization establishing the atomic basis for bioactivity is required.

Furthermore, in past years bioactive organic−inorganic hybrids with mechanical behavior closer to bone have been synthesized in order to expand the clinical applications of glasses. With this purpose several hybrid systems were investigated including the CaO−SiO_2−poly(dimethylsiloxane) (PDMS) system.[5] The effects of certain synthesis parameters in the in vitro bioactivity of these materials were studied,[5−7] but again, the effect of the hybrid nanostructure in their bioactivity needs to be clarified.

However, it is a well-known fact that calcium does exert a positive effect in the bioactive behavior, but such effect has not been satisfactorily explained yet.

To explain the role of calcium in the in vitro bioactivity of glasses and hybrids and why phosphorus in sol−gel glasses slows down their initial reactivity but then speeds up the CHA formation rate,[8] in the present study high-resolution transmission electron microscopy (HRTEM) has been performed in order to determine the nanostructure of three bioactive materials—two gel glasses, with ($\mathbf{G_{Si-Ca-P}}$) and without ($\mathbf{G_{Si-Ca}}$) phosphorus,[9] and one CaO−SiO_2−PDMS hybrid ($\mathbf{H_B}$)$^{7-}$ that will be studied in a comparative way. This technique allowed measuring the distances between [SiO_4^{4-}] tetrahedra, which are clearly lower in calcium-free materials.

Experimental Section

Two glasses in the CaO−SiO_2 and CaO−P_2O_5−SiO_2 systems and one CaO−SiO_2−PDMS organic−inorganic hybrid were syn-

* To whom correspondence should be addressed. Fax: +34 91394 1786. E-mail: vallet@farm.ucm.es.
† Facultad de Farmacia.
‡ Facultad de CC Químicas.

(1) Kokubo, T. *J. Non-Cryst. Solids* **1990**, *120*, 138.
(2) Vallet-Regí, M. *J. Chem. Soc., Dalton Trans.* **2001**, *2*, 97.
(3) Kokubo, T.; Kushitani, H.; Sakka, S.; Kitsugi, T.; Yamamuro, T. *J. Biomed. Mater. Res.* **1990**, *24*, 721.
(4) Hench, L. L. *J. Am. Ceram. Soc.* **1998**, *81*, 1705.
(5) Tsuru, K.; Aburatani, Y.; Yabuta, T.; Hayakawa, S.; Ohtsuki, C.; Osaka, A. *J. Sol-Gel Sci. Technol.* **2001**, *21*, 89.
(6) Kamitakahara, M.; Kawashita, M.; Miyata, N.; Kokubo, T. *J. Sol-Gel Sci. Technol.* **2001**, *21*, 75.
(7) Salinas, A. J.; Merino, J. M.; Hijón, N.; Martín, A. I.; Vallet-Regí, M. *Key Eng. Mater.* **2004**, *254−256*, 481.
(8) Salinas, A. J.; Martín, A. I.; Vallet-Regí, M. *J. Biomed. Mater. Res.* **2002**, *61*, 524.
(9) Vallet-Regí, M.; Izquierdo-Barba, I.; Salinas, A. J. *J. Biomed. Mater. Res.* **1999**, *46*, 560.

10.1021/cm047956j CCC: $30.25
Published on Web 03/04/2005

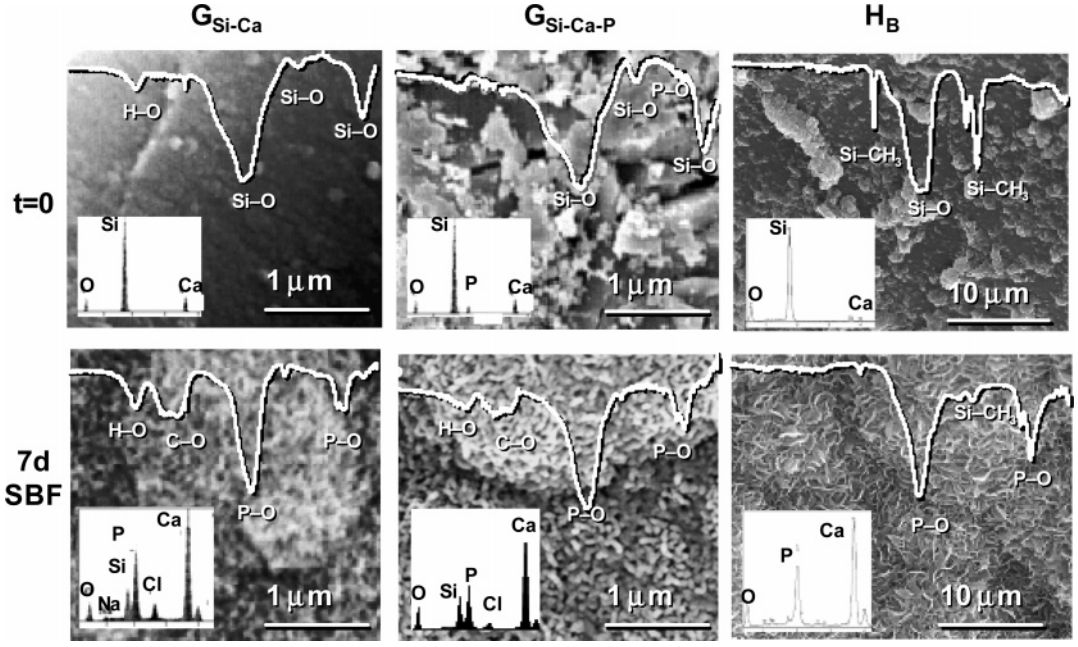

Figure 1. SEM images of the sol−gel glasses and the organic−inorganic hybrid before and after being soaked 7 days in SBF. The correspondent FTIR and EDS spectra are also included.

Table 1. Nominal Composition (wt %) of Two Sol−Gel Glasses and One Organic−Inorganic Hybrid, All Bioactive under in Vitro Conditions

	code	SiO_2	CaO	P_2O_5	PDMS−$(Si(CH_3)_2O)_n$−
glasses	G_{Si-Ca}[a]	81.1	18.9		
	$G_{Si-Ca-P}$[a]	77.9	15.3	6.8	
hybrid	H_B	24.1	2.34		73.5

[a] Subindexes in glasses refer to the elements in their composition, excluding oxygen.

thesized by sol−gel following methods previously reported.[7,9] Reactants used were calcium nitrate tetrahydrate (Fluka), tetraethoxysilane, $Si(OCH_2CH_3)_4$ (Aldrich), triethyl phosphate, $PO(OCH_2CH_3)_3$ (Aldrich), and hydroxyl-terminated PDMS, $OH[Si(CH_3)_2O]_nH$ (Aldrich, $M_n = 550$ g·mol^{-1}, $\eta = 25$ cSk). In all cases an acid catalyst was used.

Table 1 shows the nominal compositions of obtained materials. Elemental microanalysis, performed in a CHN Perkin-Elmer 2400, and X-ray Fluorescence (XRF), carried out in a Bruker S4 Explorer, showed good agreement with values in Table 1. Scanning electron microscopy (SEM) and energy dispersive X-ray spectroscopy (EDS) were performed in a JEOL 6400 microscope coupled with a LINK an 10000 device. Energy Fourier transform infrared (FTIR) spectra were collected in a ThermoNicolet Nexus equipped with a Goldengate attenuated total reflectance (ATR) stage. N_2 adsorption was carried out in a Micromeritics ASAP2010. High-resolution transmission electron microscopy (HRTEM) was performed on a JEOL 300 FEG. Image Fourier filtrations were obtained from HRTEM images by windowing the Fourier transform (FT). In the JEOL 300 FEG the energy dispersive X-ray spectroscopy (EDS) study was performed in an Oxford ISIS analyzer.

The in vitro assays of bioactivity were performed by soaking the materials in simulated body fluid (SBF), an acellular aqueous solution with inorganic ion composition almost equal to human plasma, proposed by Kokubo et al.[10] After different periods up to 7 days in SBF at 37 °C, the samples were gently rinsed with water and acetone, dried, and analyzed by FTIR, SEM, and EDS. When a new layer, mainly composed of Ca and P, and a FTIR spectrum analogous to biological apatites was formed, the sample was considered bioactive.

Results and Discussion

Assessment of the in Vitro Bioactivity of Samples. SEM micrographs of $\mathbf{G_{Si-Ca}}$, $\mathbf{G_{Si-Ca-P}}$, and $\mathbf{H_B}$, before and after 7 days in SBF are shown in Figure 1. Overlapping with the images are the corresponding FTIR spectra, in the range 1800−400 cm^{-1}, as well as the EDS spectra.

For the as-prepared samples ($t = 0$), results from EDS microanalyses agree with fairly well with those calculated from theoretical values shown in Table 1. Moreover, the FTIR spectra of gel glasses show bands at 1085, 802, and 472 cm^{-1} attributable to normal vibration modes Si−O, and for $\mathbf{G_{Si-Ca-P}}$ two very low intensity bands at 597 and 565 cm^{-1} of P−O appear. In the FTIR spectrum of $\mathbf{H_B}$ hybrid that contains PDMS the bands at 1262, 846, and 798 cm^{-1} of $Si-CH_3$ are also present.

After 7 days in SBF the situation has dramatically changed. SEM micrographs show that the three samples were coated by a new layer constituted by aggregates of particles. The EDS analysis points out that in all cases the layer is mainly composed of Ca, P, and O, although small proportions of Cl and Na ions, the more abundant components of SBF, were also detected. For $\mathbf{G_{Si-Ca}}$ and $\mathbf{G_{Si-Ca-P}}$ glasses the presence of Si in the EDS spectra could come from the glass substrate as a consequence of the small thickness of the layer. Regarding the FTIR spectra, bands at 604 and 567 cm^{-1}, usually assigned to the phosphate group in a crystalline environment, plus another one at 1035 cm^{-1}, also attributable to phosphate, are present.[11] In addition, bands assignable to carbonate are observed in the FTIR spectra of glasses. All these data combined allow us to consider that an apatite-

(10) Kokubo, T.; Kushitani, H.; Sakka, S.; Kitsugi, T.; Yamamura, Y. *J. Biomed. Mater. Res.* **1990**, *24*, 721.

(11) Elliott, J. C. *Structure and Chemistry of the Apatites and other Calcium Orthophosphates*; Elsevier: Amsterdam, 1994; p 59.

like phase was formed onto the surfaces of the three materials after 7 days in SBF and, consequently, that they have in vitro bioactivity. Although at this time the situation can be considered similar for both glasses, some differences were detected in the formation of the calcium phosphate layer. Thus, $\mathbf{G_{Si-Ca}}$ showed the highest reactivity during the first 24 h in SBF, but then the CHA crystallization was slower than that for the P-containing glass, $\mathbf{G_{Si-Ca-P}}$. On the other hand, the in vitro formation of CHA on $\mathbf{H_B}$ hybrid was comparatively delayed with respect to the sol−gel glasses because both the morphology of the particles detected by SEM and the absence of carbonate bands in the FTIR spectra of the hybrid suggest the presence of octacalcium phosphate, often considered an intermediate step between the amorphous phosphate and CHA. These differences in the in vitro behavior of the three studied materials will be explained with the nanostructural characterization of the as-prepared samples.

Nanostructural Characterization of As-Prepared Samples. The experimental HRTEM image of $\mathbf{G_{Si-Ca}}$ (Figure 2a) shows the typical contrast of an amorphous material. The Fourier transform (FT) is obtained from the digitized HRTEM image (Figure 2b), where the broad diffused scattering and rings at low angle are indicative of the amorphous nature. By placing small windows around all fundamental spots in the FT a subsequent inverse Fourier transformation strongly suppress high-frequency nonperiodic noise from the image. The obtained Fourier-filtered image (Figure 2c) clearly shows different areas presenting strong dots ordered in crystalline blocks, as marked by a rectangle. The projected potential of a crystal depends mainly on the species of the constituent elements. The electrostatic potential in a crystal composed of light elements is generally low. On the other hand, the columns along which heavy atoms densely array are seen as dark spots. Since the image contrast is proportional to the projected potential, it is possible to discriminate the atomic species. On the basis of this information it can be assumed that observed dots in Figure 2c are correlated to the positions of tetrahedral [SiO_4^{4-}] units; an average distance between these tetrahedra of 0.53 nm is measured. On the other hand, local quasi-crystalline blocks, marked by circles, also appear. Moreover, some kind of chain connecting these different blocks is also observed.

A more complicated nanostructure appears for the ternary glass with phosphorus $\mathbf{G_{Si-Ca-P}}$. The HRTEM image (Figure 3a) shows a glassy matrix containing some crystalline domains, which are, in fact, single crystals grown both on and from the surface of the glass. The Fourier-filtered HRTEM image of the amorphous matrix (Figure 3b) shows similar structural features but shorter interplanar distances (0.36 nm) than those observed in $\mathbf{G_{Si-Ca}}$ (0.53 nm). Such short distances suggest that Ca was not into the glass network. EDS microanalysis confirms that amorphous areas are Ca free and indicates that P is only present in ordered areas, suggesting that P incorporation gives rise to the formation of crystallized phosphates containing the Ca ions. Figure 3c,d reveals the existence of P-rich crystalline areas, oriented along different directions, with interplanar spacings close to 0.26 nm.

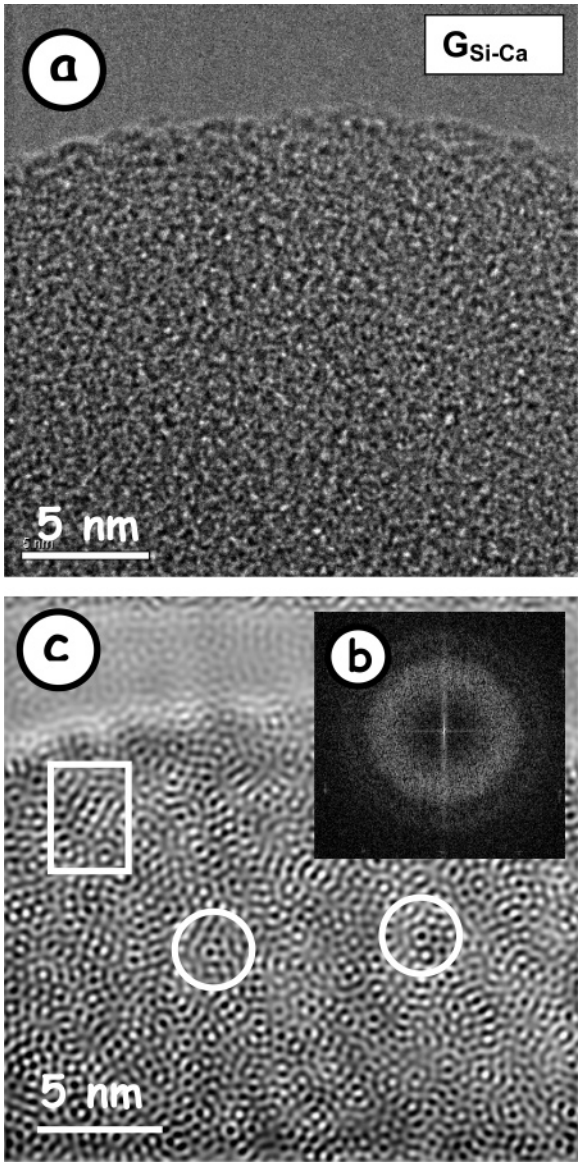

Figure 2. Electron microscopy study of $\mathbf{G_{Si-Ca}}$: (a) HTREM image, (b) corresponding FT diffraction pattern, and (c) filtered HRTEM image of the amorphous matrix. Strong dots correlating to positions of tetrahedral [SiO_4^{4-}] units, ordered in crystalline blocks, are marked by a rectangle. Local quasi-crystalline blocks are marked by circles.

Other P-rich microcrystalline areas are shown in Figure 4. Particularly interesting is the ordered area shown at the bottom right, whose FT diffraction pattern is depicted in Figure 4a and the corresponding filtered image in Figure 4b. EDS microanalysis performed on this area (Figure 4c) shows the presence of Si, P, and Ca, whereas only Ca and Si are observed in amorphous areas (Figure 4d). The pattern in Figure 4a is characteristic of rhombohedral symmetry. Note that β-tricalcium phosphate (β-TCP) crystallizes in a rhombohedral unit cell with parameters $a = 1.0439$ nm and $c = 3.7375$ nm and space group $R3c$.[12] However, inclusion of Si could lead to a decrease of symmetry since calcium silicate oxide crystallizes in a rhombohedral cell with parameters $a = 0.7135$ nm and $c = 2.5586$ nm and space group $R3m$.[13] Figure 4a,b reveals an intermediate situation since they can

(12) Dickens, B.; Schroeder, L. W.; Brown, W. E. *J. Solid State Chem.* **1974**, *10*, 232.
(13) Nishi, F.; Takeuchi, Y. *Z. Kristallogr.* **1984**, *168*, 197.

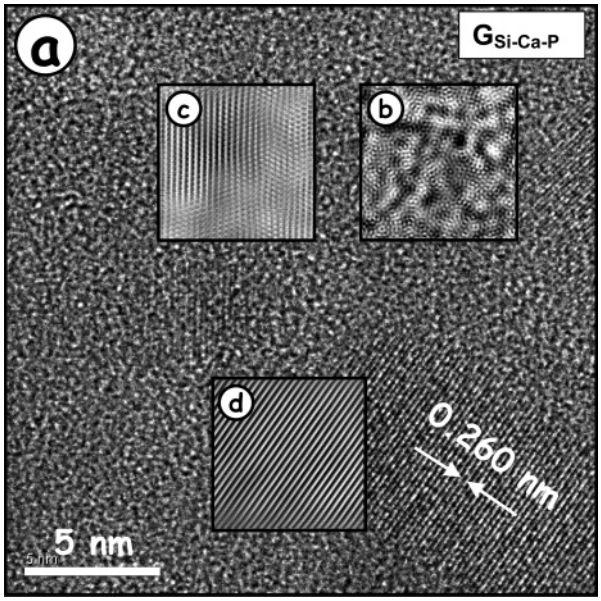

Figure 3. Electron microscopy study of $\mathbf{G_{Si-Ca-P}}$: (a) HTREM image and (b) filtered HRTEM image of the amorphous matrix. (c and d) P-Rich crystalline areas oriented along different directions.

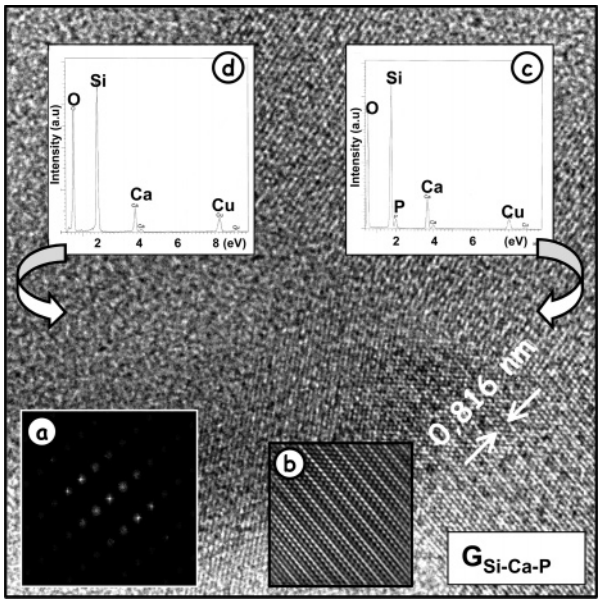

Figure 4. Electron microscopy study of a P-rich microcrystalline area of $\mathbf{G_{Si-Ca-P}}$: (a) FT diffraction pattern corresponding to the ordered area shown at the bottom and (b) filtered HRTEM image. (c) EDS microanalysis performed on the above area shows the presence of Si, P, and Ca. (d) Only Ca and Si are observed in amorphous areas.

be indexed on the basis of a *R*3*m* space group with unit cell parameters slightly smaller than those of β-TCP. Therefore, it can be concluded that inclusion of P_2O_5 in the glass leads to crystallization of Si-doped β-TCP crystallites smaller than 10 nm. Single crystals were never found to be isolated, suggesting that these calcium silicon−phosphate crystals rely on the glassy matrix for growing.

The presence of crystalline nuclei in as-prepared P-containing glass, $\mathbf{G_{Si-Ca-P}}$ visualized by HRTEM, is also inferred from other techniques such as FTIR spectroscopy (Figure 1) and N_2 adsorption (Figure 5). The FTIR spectrum of $\mathbf{G_{Si-Ca-P}}$ shows two low-intensity bands, at 604 and 567 cm^{-1}, usually assigned to phosphate in a crystalline environment.[11] These bands, together with diffuse reflections at 26°

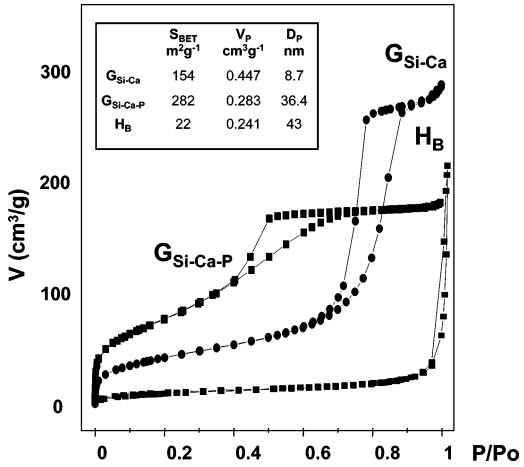

Figure 5. N_2 adsorption isotherms. (Inset) Textural parameters obtained. S_{BET} = specific surface area. V_P = pore volume. D_P = diameter of pore.

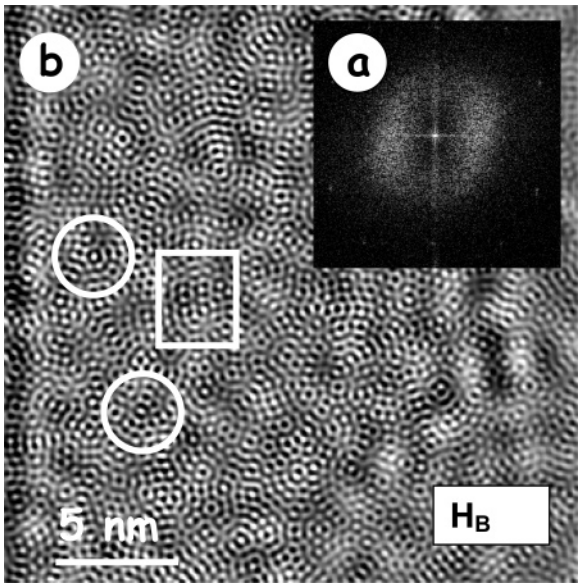

Figure 6. Electron microscopy study of $\mathbf{H_B}$: (a) filtered HRTEM image of the amorphous matrix and (b) corresponding FT diffraction pattern. Ordered crystalline blocks are marked by a rectangle, and local quasi-crystalline blocks are marked by circles.

and 32° in 2θ in the XRD pattern of this sample (not shown here), suggest the presence of some kind of crystalline phosphate nuclei in $\mathbf{G_{Si-Ca-P}}$, as also shown by HRTEM. Comparison of the textural properties of both glasses (Figure 5, inset) shows that for $\mathbf{G_{Si-Ca-P}}$ S_{BET} is higher and V_P lower. This effect could be explained considering that the P_2O_5 bond to calcium takes this element out of the glass network, producing a similar effect as when calcium was decreased in SiO_2−CaO glasses.[14]

HRTEM of $\mathbf{H_B}$ material shows the same contrast distribution observed in the glasses, suggesting similar structural features (Figure 6). The EDS microanalysis clearly shows the presence of Ca. Incorporation of Ca atoms randomly distributed into the SiO_2 cluster network can be deduced from the distances between the [SiO_4^{4-}] units 0.45 nm.

For comparison purposes a CaO−SiO_2−PDMS hybrid analogous in composition to $\mathbf{H_B}$ but not presenting in vitro

(14) Martínez, A.; Izquierdo-Barba, I.; Vallet-Regí, M. *Chem. Mater.* **2000**, *12*, 3080.

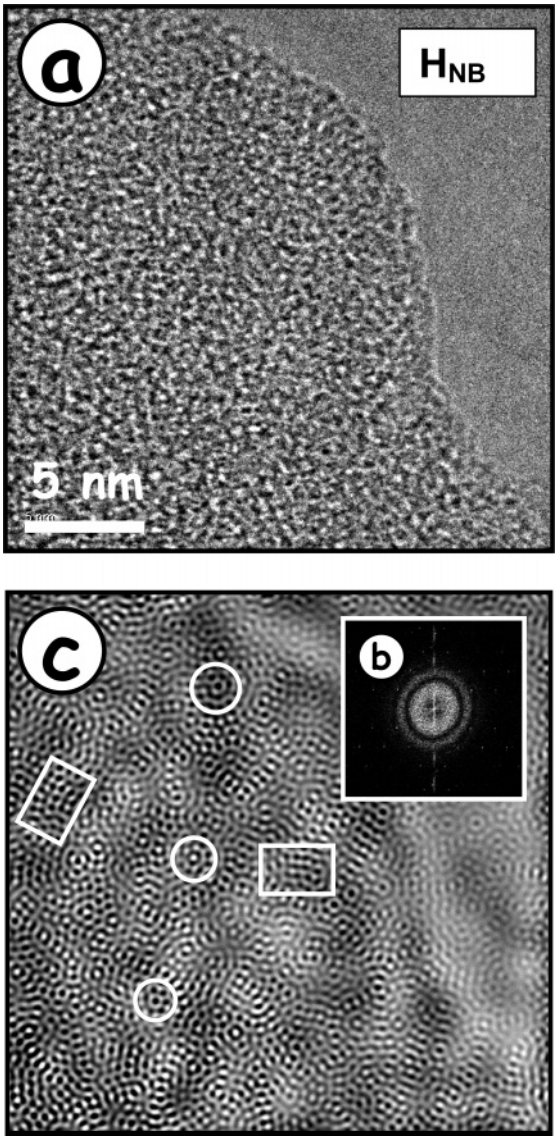

Figure 7. Electron microscopy study of a nonbioactive hybrid $\mathbf{H_{NB}}$: (a) HRTEM micrograph, (b) corresponding FT diffraction pattern, and (c) filtered HRTEM image.

bioactivity in SBF ($\mathbf{H_{NB}}$) was characterized. Actually, for the $\mathbf{H_{NB}}$ synthesis the same amounts of reactants and catalyst as for $\mathbf{H_B}$ were used, but in this case twice the amount of H_2O was used. This material does not suffer any changes after 7 days in SBF, and it was therefore considered to be nonbioactive. The filtered HRTEM image of $\mathbf{H_{NB}}$ (Figure 7a) shows the typical contrast of an amorphous material. Figure 7b shows the corresponding FT diffraction pattern. The broad diffused scattering and rings at low angle are indicative of the amorphous nature. The corresponding Fourier-filtered image (Figure 7c) shows a similar situation of that observed in $\mathbf{G_{Si-Ca}}$. Actually, an average distance of 0.39 nm between the strong dots ordered in crystalline blocks, marked by a rectangle, is measured, clearly lower than that of $\mathbf{H_B}$ (0.45 nm). Again, local quasi-crystalline blocks, marked by circles, also appear, and in addition, some kind of chain connecting these different blocks is also observed.

Differences in the in Vitro Bioactivity in SBF as a Function of the Nanostructure of Materials. At this point it is worth recalling that MacKenzie et al.[15,16] described the structure of Ca-free SiO_2-PDMS organic−inorganic phases as a SiO_2 network formed by a three-dimensional model of silica glass including linear chains of PDMS. These chains break up the continuity of the SiO_2 block network, modifying the mechanical properties of silica. It is worth stressing that EDS data indicate that, different from $\mathbf{H_B}$, Ca has not been incorporated into the $\mathbf{H_{NB}}$ network. Accordingly, a tentative structural model can be proposed as being formed by a block framework of $[SiO_4^{4-}]$ tetrahedra, spaced by a distance of ca. 0.39 nm, involving a "disordered" distribution of crystalline nanodomains, alternating with noncrystalline domains, giving rise to a random distribution of SiO_2 "clusters" connected by $-(Si(CH_3)_2O)_n-$ chains of different lengths.

The N_2 adsorption/desorption isotherms for $\mathbf{G_{Si-Ca}}$, $\mathbf{G_{Si-Ca-P}}$, and $\mathbf{H_B}$ (Figure 5) correspond to type IV in the BDDT classification.[17] For $\mathbf{G_{Si-Ca-P}}$ the hysteresis loop corresponds to a mesoporous material (2 nm $< D_P <$ 50 nm) with narrow necked pores, whereas for $\mathbf{G_{Si-Ca}}$ the loop is characteristic of cylindrical pores with both sides open. Comparing the textural parameters of glasses and hybrids (Figure 5 inset) it can be observed that PDMS leads to a large decrease in the specific surface area and porosity of hybrids.

According to the nanostructural characterization it can be established that the different rates of positive bioactive response of two gel glasses is strongly related with its nanostructure, since distances between the $[SiO_4^{4-}]$ tetrahedra decrease when Ca is not into the glass network and phosphorus is bonded to calcium, forming silicon-doped calcium phosphate nuclei with size lower than 10 nm. It must be pointed out that in P-free glasses, such as $\mathbf{G_{Ca-Si}}$, a quicker initial reactivity in SBF was found, whereas in P-containing glasses, such as $\mathbf{G_{Ca-Si-P}}$, a higher crystallization rate of CHA was observed.[8]

On the basis of the characterization of glasses different CHA formation mechanisms upon soaking in SBF can be proposed for each glass. In $\mathbf{G_{Si-Ca}}$ bioactivity is controlled by the rapid exchange of calcium in the glass network by protons in solution forming silanol (Si−OH) groups, which attract calcium and phosphorus in SBF to form an amorphous calcium phosphate. Afterward, a relatively long period is required for the in vitro crystallization of CHA. However, for $\mathbf{G_{Si-Ca-P}}$ glass the silanol concentration is lower, retarding the amorphous calcium phosphate formation, but the presence of the mentioned nanocrystals increases the CHA crystallization rate. This effect could be explained by the solubility of the nanocrystals in glass under in vitro conditions, which will increase the ionic force and the supersaturation of the solution and the possible role of these nanocrystals as nucleation centers.

$\mathbf{H_B}$ and $\mathbf{H_{NB}}$ hybrids also exhibit different kinetics of bioactive response, which is related both to nanostructure and chemical composition. In fact, once again distances between $[SiO_4^{4-}]$ tetrahedra suggest that calcium is only present in the hybrid network of $\mathbf{H_B}$, as confirmed by XRF and EDS. Thus, although in the synthesis of both hybrids

(15) Hu, Y.; Mackenzie, J. D. *J. Mater. Sci.* **1992**, *27*, 4415.
(16) Mackenzie, J. D.; Huang, Q.; Iwamoto, T. *J. Sol-Gel Sci. Technol.* **1996**, *7*, 151.
(17) Gregg, J. S.; Sing, K. S. W. *Adsorption, Surface Area and Porosity*; Academic Press: New York, 1982; p 1.

the same amount of reactants was used, the different hydrolysis conditions facilitate or inhibit the incorporation of calcium to the hybrid, playing an essential role in its bioactivity.

Therefore, common features of the bioactive behavior of glasses and organic−inorganic hybrids are that inclusion of calcium into the SiO_2 network increases the CHA formation rate and addition of a third component, P_2O_5 in glasses and PDMS in hybrids, hinders incorporation of calcium in the material and consequently the in vitro bioactivity. However, each family of compounds reacts differently to the presence of this third component. In P-containing glasses nanocrystals of silicon-doped calcium phosphate are formed, but in hybrids the hydrophobic quality of PDMS restricts the calcium inclusion just to the SiO_2-rich zones and, sometimes, impedes this inclusion, producing hybrids unable to form the CHA layer under in vitro conditions.

Acknowledgment. Financial support of CICYT, Spain, through research project MAT 2002-0025 is acknowledged. The authors also thank C.A.I. X-ray diffraction, UCM, and C.A.I. Electron Microscopy Center, UCM, for technical and professional assistance.

CM047956J